On the influence of frequency and width of an ultrasonic bounded beam in the investigation of materials: Study in terms of heterogeneous plane waves

K. Van Den Abeele[a] and O. Leroy
Interdisciplinary Research Center, K.U.L. Campus Kortrijk, B-8500 Kortrijk, Belgium

(Received 23 September 1992; accepted for publication 12 January 1993)

Theoretically obtained three-dimensional plots showing the behavior of the reflection coefficient for heterogeneous plane waves upon arbitrary layered media as function of incidence angle and heterogeneity, supply valuable information for the investigation of the reflector when using bounded ultrasonic beams. The presence of leaky interface modes and their angular positions for a specific sample are determined by the fd products (frequency times thickness) of the constituent layers. Deformations of the reflected and transmitted bounded beam profiles and the contribution of surface wave radiation (leaking energy) at vibrational mode angles are governed by the fW product (frequency times beamwidth). For a given layered medium, optimum conditions for observing particular mode vibrations and large deformations of reflected ultrasonic profiles can be predicted theoretically.

PACS numbers: 43.35.Zc

INTRODUCTION

Nonspecular reflectivity of ultrasonic bounded beams incident from a liquid onto a layered medium has always been brought in close connection to the generation of surface waves inside the medium. Bertoni and Tamir[1] suggested that the deformation of the reflected beam at a liquid/solid interface must be considered to be composed of a specular reflected beam and a second field which corresponds to a leaky Rayleigh wave field situated at large distances from the beam incidence along the interface. Plona *et al.*[2] and Pitts *et al.*[3] noted similarities between the liquid/solid interface and the liquid/solid plate/liquid medium and applied the theory of Bertoni and Tamir qualitatively to the latter case. Extensions of these theoretical models resulted in a general description of ultrasonic nonspecular reflection and transmission effects for layered media,[4–8] in which bounded beams are described by Fourier analysis.

Leaky Lamb waves are said to cause deformed and displaced reflected and transmitted fields. Because these leaky surface waves carry important information about the elastic properties of the reflector, their study has become very useful in nondestructive evaluation techniques especially in the field of acoustic microscopy. By detecting and analyzing strong leaky waves, the elastic properties of the reflector can be obtained.[9] Therefore, it is important to know which incident angles under what conditions produce strong leaky waves.

De Billy and Molinero[10,11] observed in their experiments that symmetrical modes can be missing at expected Lamb wave angles (θ_{Lw}) near the longitudinal critical angle due to an effect of weak coupling between two media. An attempt to explain this phenomenon links the ultrasonic beamwidth W and the imaginary part of the wavenumber solution of the characteristic Lamb wave equations $\mathrm{Im}(k_{Lw})$ to a parameter

$$h = W\,\mathrm{Im}(k_{Lw})/(2\cos\theta_{Lw}),$$

which is highly connected to the amplitude variation in the reflected profile. Plots in Ref. 4 show that this parameter is almost zero for any symmetrical mode near the longitudinal critical angle, which means that the surface wave radiation is very weak for this angle range and that, as a consequence, it will be impossible to observe nonspecular reflection effects.

In this article, we investigate the influence of the parameters f and W (frequency and beamwidth) of a Gaussian ultrasonic wave on a solid plate of thickness d immersed in a liquid bath and we will determine optimum conditions for excitation of leaky waves. Especially the product fW appears to be extremely important in the generation of the surface waves and the observance of nonspecular effects. The method presently used is based on the inhomogeneous wave description of a bounded beam profile suggested by Claeys *et al.*,[12] and the recent findings of Van Den Abeele *et al.*[13,14] about the separation of the reflected profile and the Lamb wave component in the liquid.

We will first recall the concept of heterogeneous waves and their use in the decomposition of a bounded beam profile. Properties of the reflection and transmission coefficients of such waves suggest a separation of the scattered fields in reflection and transmission into an attendant profile and an additional energy flow in the liquid. In the second part, we restrict ourselves to the incidence of a Gaussian ultrasonic beam on a plate immersed in water and we investigate the influence of two experimentally adjustable parameters, namely frequency and beamwidth, in relation to the plate thickness. Theoretically calculated examples illustrate the possibility to predict an optimal beamwidth–frequency combination with which to generate

[a]Aspirant of the Belgian National Foundation for Scientific Research.

 0001-4966/93/052688-12$06.00

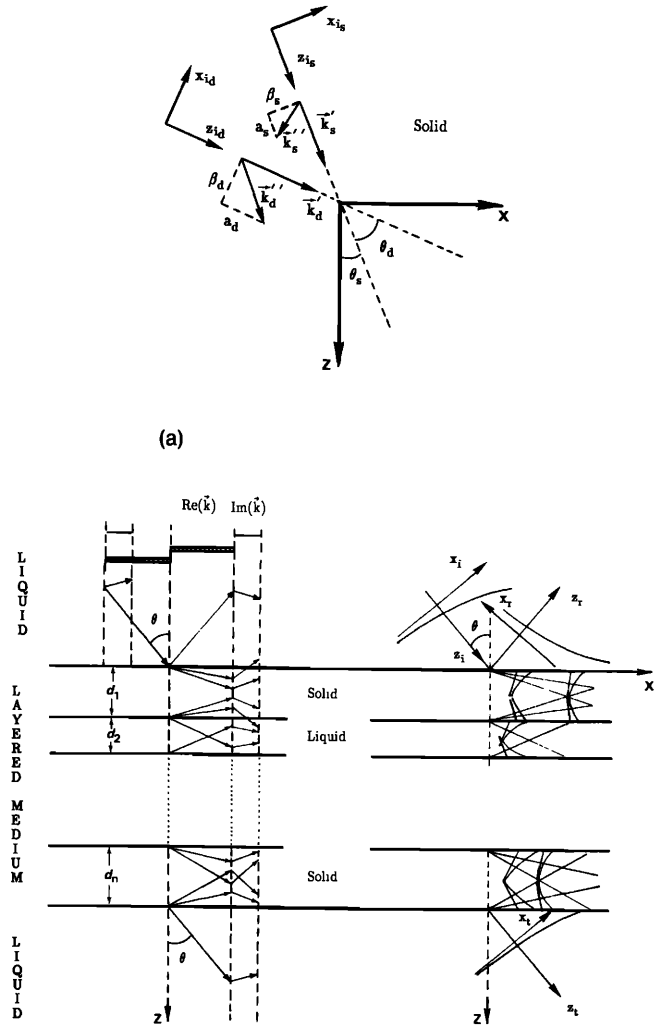

FIG. 1. (a) Geometry of dilatational and shear horizontal complex harmonic waves in a solid by means of bivectors. (b) General geometrical representation of complex harmonic wave scattering in a layered medium.

strong leaky Lamb waves. Moreover, for samples of different thickness, one can adjust frequency and beamwidth in such a way that approximately the same features occur for each experimental situation. These results can be of great importance in the field of acoustic microscopy and for laboratory experiments on scale models.

I. BOUNDED BEAM SCATTERING AT LAYERED MEDIA IN TERMS OF HETEROGENEOUS WAVES: GENERAL APPROACH

When no shear-horizontal waves are to be taken into account, the general mathematical representation of the particle displacements can be chosen independent of y and are expressed in terms of two potential functions of the following form [for the geometry, see Fig. 1(a)]:

$$\Phi_m(x,z,t)=A_m \exp[i(\mathbf{k}_m\cdot\mathbf{r}-\omega t)], \quad m=d \text{ or } s, \tag{1}$$

in which ω is the circular frequency, A_m is the complex amplitude, and $\mathbf{k}_m$ is a complex valued vector satisfying

$$\mathbf{k}_m\cdot\mathbf{k}_m=\kappa_m^2=(k_{0m}+ia_{0m})^2, \quad m=d \text{ or } s, \tag{2a}$$

with κ_d and κ_s the complex wave numbers for the dilatational ($m=d$) and shear-vertical ($m=s$) component, respectively, related in a first-order approximation to the medium constants v_m (velocity) and α_m (attenuation) by

$$k_{0m}=\omega/v_m \quad \text{and} \quad a_{0m}=\omega^2\alpha_m, \quad m=d \text{ or } s. \tag{2b}$$

Using the bivector formalism,[15–17] we write $\mathbf{k}_m$ as a complex combination of two real-valued vectors $\mathbf{k}'_m$ and $\mathbf{k}''_m$, the former defining the phase velocity and the angle θ_m with respect to a fixed z direction, and the latter connected to attenuation properties of the wave in the direction of propagation and in the direction perpendicular to it. In a coordinate system (x_{i_m},z_{i_m}) obtained from the (x,z) system by an in plane rotation over an angle θ_m so that the z_{i_m} axis is pointing toward the direction of propagation, the potential functions take on the following form:

$$\Phi_m(x_{i_m},z_{i_m},t)=A_m \exp(\beta_m x_{i_m})\exp(-a_m z_{i_m}) \times\exp[i(k'_m z_{i_m}-\omega t)], \quad m=d \text{ or } s, \tag{3}$$

with k'_m the length of $\mathbf{k}'_m$, a_m the projection of $\mathbf{k}''_m$ on the z_{i_m} axis, and β_m the projection of $\mathbf{k}''_m$ on the negative x_{i_m} axis.

Equation (3) is the mathematical description of a plane harmonic wave (dilatational or shear vertical depending on m) propagating in z_{i_m} direction with phase velocity ω/k'_m while decaying by an amount a_m which corresponds to the attenuation of the wave in the propagation direction. Furthermore, this wave has an amplitude variation with exponential behavior along its wave fronts represented by the heterogeneity characteristic β_m.

For given frequency and incidence direction θ_m, the heterogeneity β_m fixes the possible combinations of phase velocity ω/k'_m and attenuation a_m in the direction of propagation by means of one of the complex dispersion relations (2), for dilatational ($m=d$) and shear-vertical ($m=s$) waves, respectively. These (real and positive) values are simply and solely determined by the given medium constants $\{v_d,\alpha_d\}$ and $\{v_s,\alpha_s\}$ as is required by condition (2):

$$\left.\begin{aligned} k'^2_m-a^2_m-\beta^2_m&=k^2_{0m}-a^2_{0m}\\ k'_m a_m&=k_{0m}a_{0m}\end{aligned}\right\} \quad m=d \text{ or } s. \tag{4}$$

This means that each heterogeneous wave can be characterized by a multiplet $(k_{0m},a_{0m},k'_m,a_m,\beta_m,\theta_m)$, where m distinguishes between dilatational and shear-vertical waves. The first two constants specify the medium characteristics and the frequency, the three following parameters determine the nature of the wave satisfying Eq. (4), and θ_m defines the angle between the propagation direction and any fixed direction identified as z axis of an orthogonal coordinate system.

Let us suppose now that a heterogeneous wave characterized by its multiplet $(k_{0m},a_{0m},k'_m,a_m,\beta_m,\theta_m)$ is incident at an angle θ_m on a layered medium with plane parallel interfaces between the different viscoelastic isotropic

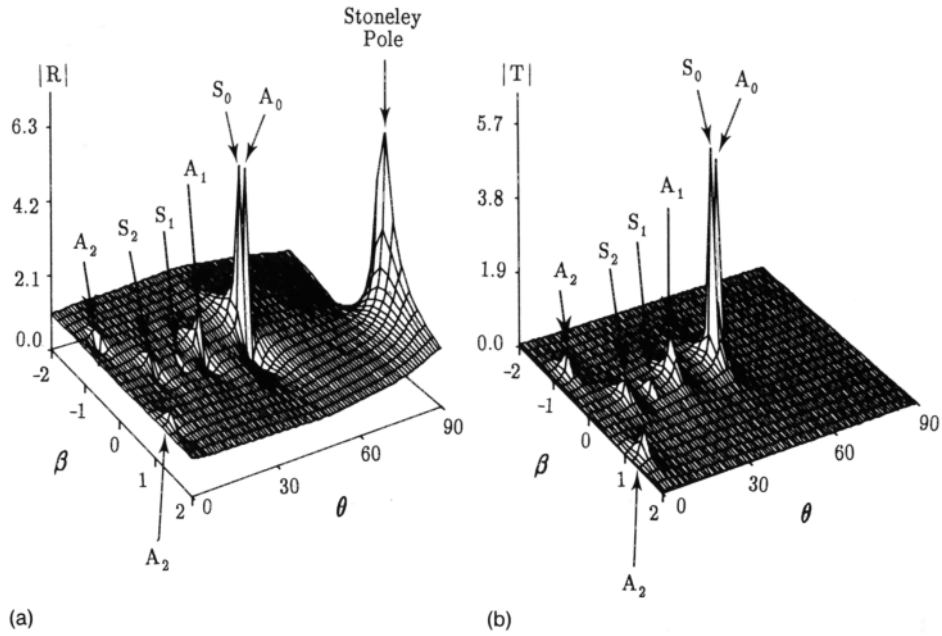

FIG. 2. Three-dimensional representation of calculated heterogeneous wave reflection and transmission coefficients as a function of angle of incidence and heterogeneity for a viscous brass plate of 1.6-mm thickness insonified in water at 2-MHz frequency. The locations of the plate modes are indicated by an arrow.

layers. In general, this wave will generate a number of dilatational and shear-vertical heterogeneous waves propagating up and downward inbetween the boundaries of each layer [Fig. 1(b)]. For each layer (solid or liquid), the nature of these waves, their directions with respect to the z axis and their relative amplitudes immediately follow from the facts that, first of all, the complex dispersion relations for the new propagation medium are to be satisfied and that, second, certain conditions are required at each boundary in order to obtain continuity. More precisely, the necessity of invariability of the wave vector x coordinate $k_x = k'_m \sin\theta_m + ia_m \sin\theta_m - i\beta_m \cos\theta_m$, leading to the generalized Snell–Descartes laws, together with the new dispersion relations brings up a set of four real (nonlinear) equations in the four unknown characteristics which define the nature and the direction of each generated complex harmonic wave. Techniques to solve this set are described for several cases by Deschamps *et al.*[15] The determination of the relative amplitudes of the scattered heterogeneous waves in each layer of the sample can be described by an extension of Brekhovskikh's theory for complex wave numbers and complex x and z wave-vector projections.[18] An example illustrating the behavior of the calculated reflection ($|\mathbf{R}|$) and transmission moduli ($|\mathbf{T}|$) as function of heterogeneity and incidence angle of a complex harmonic longitudinal wave insonifying a brass plate immersed in water is shown by the surfaces in Fig. 2.

Peaks of the reflection and transmission moduli clearly show (β,θ) combinations for which the denominator of **R** and **T** tends toward zero. These locations exactly correspond to the complex x components of the wave numbers of the leaky surface modes (symmetric and asymmetric leaky Lamb waves in this case). Furthermore, if $k_{x_{\text{pole}}}$ is such a pole of **R** (or **T**), the full character (k_{Lw}, a_{Lw}, and β_{Lw}) and the right angle θ_{Lw} of the corresponding leaky wave components in the liquid (with "medium constants" $k_{0_{\text{liq}}}$ and $a_{0_{\text{liq}}}$) at both sides of the plate can be determined by solving:

$$k_{\text{Lw}} \sin\theta_{\text{Lw}} = \text{Re}(k_{x_{\text{pole}}}),$$

$$a_{\text{Lw}} \sin\theta_{\text{Lw}} - \beta_{\text{Lw}} \cos\theta_{\text{Lw}} = \text{Im}(k_{x_{\text{pole}}}), \tag{5}$$

$$k_{\text{Lw}}^2 - a_{\text{Lw}}^2 - \beta_{\text{Lw}}^2 = k_{0_{\text{liq}}}^2 - a_{0_{\text{liq}}}^2, \quad k_{\text{Lw}} a_{\text{Lw}} = k_{0_{\text{liq}}} a_{0_{\text{liq}}}.$$

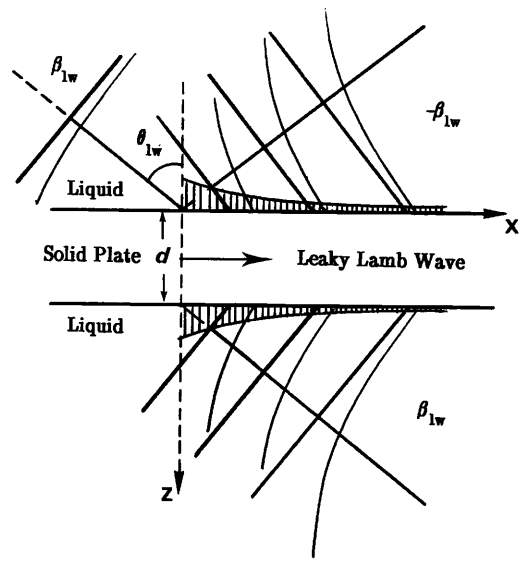

FIG. 3. The leaky Lamb wave and its energy components at both sides of a plate in water: a well-defined combination of complex harmonic waves.

TABLE I. Relative amplitudes A_n of the heterogeneous waves used in the decomposition of a Gaussian profile (n,A_n).

0	−0.101 585*E*00	8	−0.253 160*E*02	16	−0.963 892*E*−05	24	−0.116 916*E*−15	32	−0.112 837*E*−30
1	0.219 627*E*01	9	0.801 411*E*01	17	0.696 972*E*−06	25	0.264 569*E*−17	33	0.695 937*E*−33
2	−0.209 847*E*02	10	−0.202 240*E*01	18	−0.432 819*E*−07	26	−0.518 114*E*−19	34	−0.347 116*E*−35
3	0.775 777*E*02	11	0.414 019*E*00	19	0.231 621*E*−08	27	0.875 971*E*−21	35	0.136 344*E*−37
4	−0.141 464*E*03	12	−0.697 106*E*−01	20	−0.107 098*E*−09	28	−0.127 424*E*−22	36	−0.405 503*E*−40
5	0.155 761*E*03	13	0.976 173*E*−02	21	0.428 722*E*−11	29	0.158 749*E*−24	37	0.857 345*E*−43
6	−0.115 878*E*03	14	−0.114 722*E*−02	22	−0.148 771*E*−12	30	−0.168 354*E*−26	38	−0.114 701*E*−45
7	0.623 143*E*02	15	0.114 003*E*−03	23	0.447 807*E*−14	31	0.150 771*E*−28	39	0.729 231*E*−49

We can interpret the multiplet $(k_{0_{\text{liq}}},a_{0_{\text{liq}}},k_{\text{Lw}},a_{\text{Lw}},\beta_{\text{Lw}},\theta_{\text{Lw}})$ with $0\leqslant\theta_{\text{Lw}}<\pi/2$ as the characterization of the particular incident heterogeneous wave for which symmetric or antisymmetric Lamb waves are traveling inside the plate with velocity $\omega/\text{Re}(k_{x_{\text{pole}}})$ along the x direction. These waves are leaking part of their energy through the interfaces separating the liquid half-spaces from the solid plate at both sides (Fig. 3). In reflection this energy flow is fully characterized by the heterogeneous wave $(k_{0_{\text{liq}}},a_{0_{\text{liq}}},k_{\text{Lw}},a_{\text{Lw}},-\beta_{\text{Lw}},\pi-\theta_{\text{Lw}})$ and by $(k_{0_{\text{liq}}},a_{0_{\text{liq}}},k_{\text{Lw}},a_{\text{Lw}},\beta_{\text{Lw}},\theta_{\text{Lw}})$ in transmission. This proves that the excitation of surface waves can be explained as a pure reflection/transmission phenomenon of heterogeneous waves.

To account properly for the bounded character of an experimentally used ultrasonic beam, Claeys and Leroy[12] introduced a method based on the decomposition of its profile into a finite discrete series of heterogeneous waves propagating in one specific direction. In order to explicitly show the close connection between bounded beam profile deformation and surface or plate mode excitation, Van Den Abeele and Leroy[13,14] extended the preliminary approach to a more general approximation using complex harmonic waves with both decaying $(\beta\geqslant 0)$ and exponentially growing $(\beta\leqslant 0)$ amplitude variations along the wave fronts, leading to the possibility to separate the attendant reflected field from the leaky surface wave components.

In the present paper, we will focus our attention on the reflection and transmission of a Gaussian beam of half-width W upon a plate immersed in water (Fig. 4). As water is the medium in which the incident, reflected and transmitted beam profiles will be observed, we are only concerned about incident longitudinal waves. Therefore, we can omit the subscript d without being mistaken. The index n used throughout the rest of this paper from now on stands for the summation index in the finite decomposition of the ultrasonic field. The method of Claeys and Leroy provides a reasonable approximation of the symmetrical Gaussian profile for

$$\exp\left[-\left(\frac{x_i}{W}\right)^2\right]=\sum_{n=-39}^{+39}A_n e^{\beta_n x_i}, \tag{6}$$

with

$$\beta_n=-\beta_{-n}=n/1.9W, \quad \text{for} \quad n:-39\cdots 39, \tag{7}$$

and with coefficients A_n $(=A_{-n})$ given in Table I. An important remark is that the heterogeneities β_n of the different waves in the decomposition are inversely proportional to the width of the beam profile while the coefficients A_n are independent of the width, so that they can be tabulated beforehand which reduces the computing time.

Because of linearity, the amplitude and phase distribution of the reflected and transmitted profile for any angle of incidence θ can be found by multiplying each heterogeneous wave (index n) by its complex valued reflection/transmission coefficient:

$$\mathbf{R}(k_n'\sin\theta+ia_n\sin\theta-i\beta_n\cos\theta)$$

and

$$\mathbf{T}(k_n'\sin\theta+ia_n\sin\theta-i\beta_n\cos\theta).$$

In earlier work, we showed that the reflected field contains all possible information about beam deformations and generation of leaky surface waves.[13,14] Without affecting the energy balance, we can break apart the reflected (as well as the transmitted) field in two separate components with significant physical meaning. Depending on the sign of the heterogeneity parameter β_{Lw} of the leaky wave solution $(k_{0_{\text{liq}}},a_{0_{\text{liq}}},k_{\text{Lw}},a_{\text{Lw}},\beta_{\text{Lw}},\theta_{\text{Lw}})$ for angles of incidence θ in the neighborhood of θ_{Lw}, these components can be mathematically described by

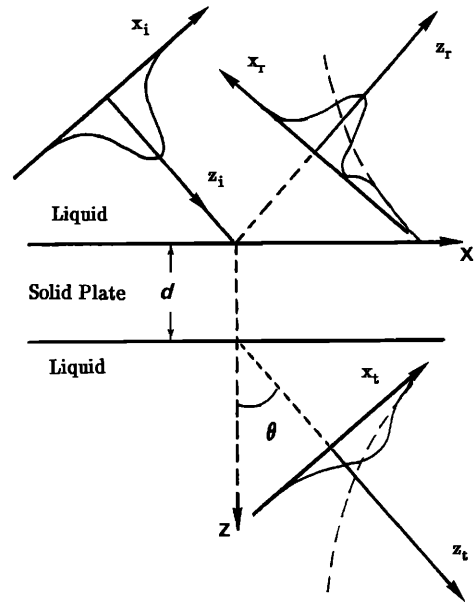

FIG. 4. Geometry of the reflection and transmission phenomena for bounded beams.

$$\left.\begin{aligned} &A_0 R[(k_x)_0] + 2\sum_{n=1}^{+39} A_n R[(k_x)_n] e^{-\beta_n x_r} \\ &\sum_{n=1}^{+39} A_n \{R[(k_x)_{-n}] e^{\beta_n x_r} - R[(k_x)_n] e^{-\beta_n x_r}\} \end{aligned}\right\} \begin{aligned} &\text{for } \beta_{\mathrm{Lw}} < 0, \\ &\end{aligned} \quad \begin{aligned} &(8a) \\ &(8b) \end{aligned}$$

or by

$$\left.\begin{aligned} &A_0 R[(k_x)_0] + 2\sum_{n=1}^{+39} A_{-n} R[(k_x)_{-n}] e^{\beta_n x_r} \\ &\sum_{n=1}^{+39} A_n \{R[(k_x)_n] e^{-\beta_n x_r} - R[(k_x)_{-n}] e^{\beta_n x_r}\} \end{aligned}\right\} \begin{aligned} &\text{for } \beta_{\mathrm{Lw}} > 0. \\ &\end{aligned} \quad \begin{aligned} &(9a) \\ &(9b) \end{aligned}$$

The first component in each case represents the attendant reflected profile, almost exactly to what Fourier analysis predicts, while the second one can be associated with the presence of a leaky wave and is connected to the extension of the trailing field. In all figures of the next section, the attendant reflected profile is visualized by the dotted line, the leaky wave component into the liquid by the dashed line and the original incident profile as a reference by the full line. Above each profile illustration, the moduli of the reflection coefficient for the different complex harmonic waves in the decomposition [Eq. (6)] are shown as a function of their heterogeneity characteristic. For a more detailed explanation and examples for Rayleigh, Lamb, and Stoneley wave generation in reflection (and transmission) of bounded beams we refer to Refs. 13 and 14.

II. INFLUENCE OF BEAMWIDTH PARAMETER, FREQUENCY AND PLATE THICKNESS ON BOUNDED BEAM SCATTERING AND ON THE GENERATION OF LEAKY SURFACE WAVES

In this investigation, we suppose that three plates of the same viscoelastic material "brass" (identical material constants: $v_d = 4410$ m/s, $\alpha_d = 30 \times 10^{-18}$ s^2/mm, $v_s = 2150$, m/s, $\alpha_s = 130 \times 10^{-18}$ s^2/mm, $\rho = 8.6$) with different thicknesses are available: plate 1 is 1 mm thick; plate 2: 2.5 mm; and plate 3 has a thickness of 5 mm.

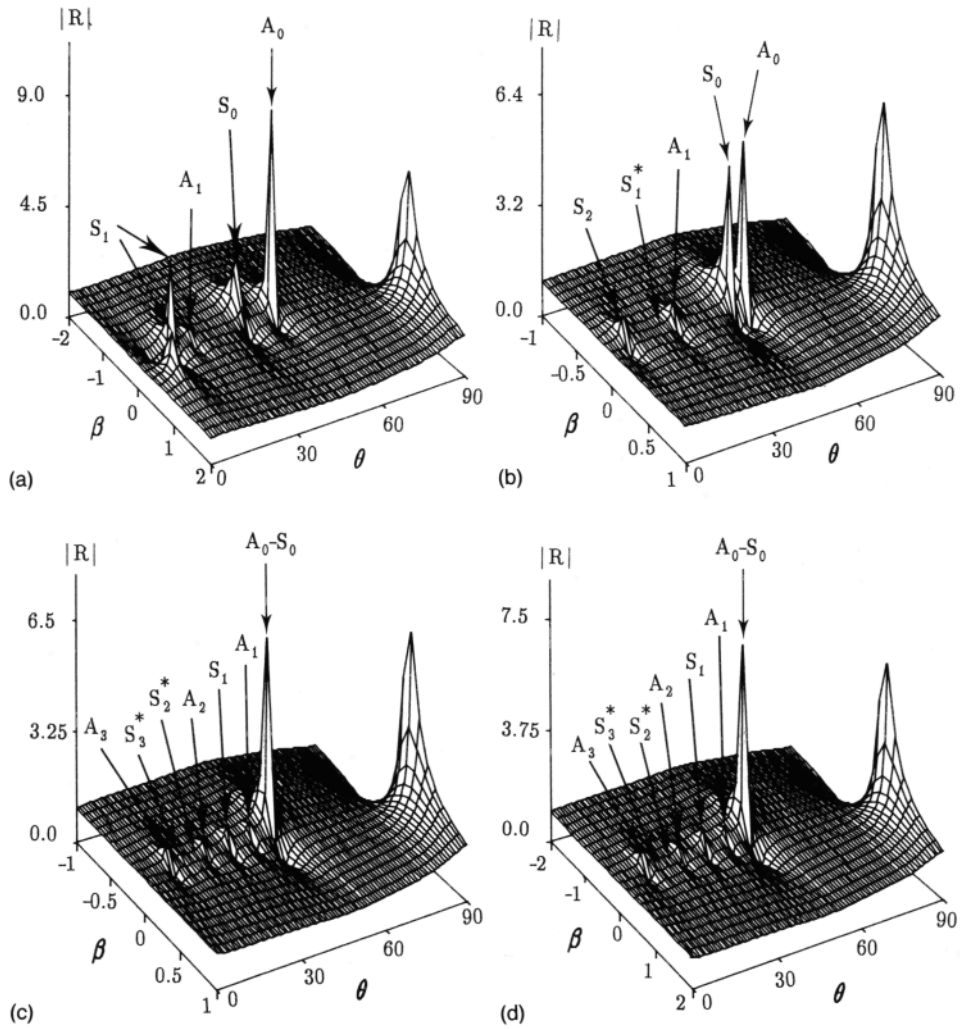

FIG. 5. Three-dimensional representations of calculated heterogeneous wave reflection coefficients as a function of angle of incidence and heterogeneity for different frequency-thickness combinations in the case of a viscous brass plate in water. (a) $fd = 2.0$ MHz mm ($f = 2$ MHz, $d = 1$ mm), (b) $fd = 2.5$ MHz mm ($f = 1$ MHz, $d = 2.5$ mm), (c) $fd = 5.0$ MHz mm ($f = 1$ MHz, $d = 5$ mm) (d) $fd = 5.0$ MHz mm ($f = 2$ MHz, $d = 2.5$ mm), (e) $fd = 5.0$ MHz mm ($f = 5$ MHz, $d = 1$ mm), (f) $fd = 10.0$ MHz mm ($f = 5$ MHz, $d = 2$ mm), (g) $fd = 2.5$ MHz mm: The S_1-mode location. The locations of all plate modes are indicated by an arrow. Modes which are invisible due to the chosen grid are marked with an asterisk.

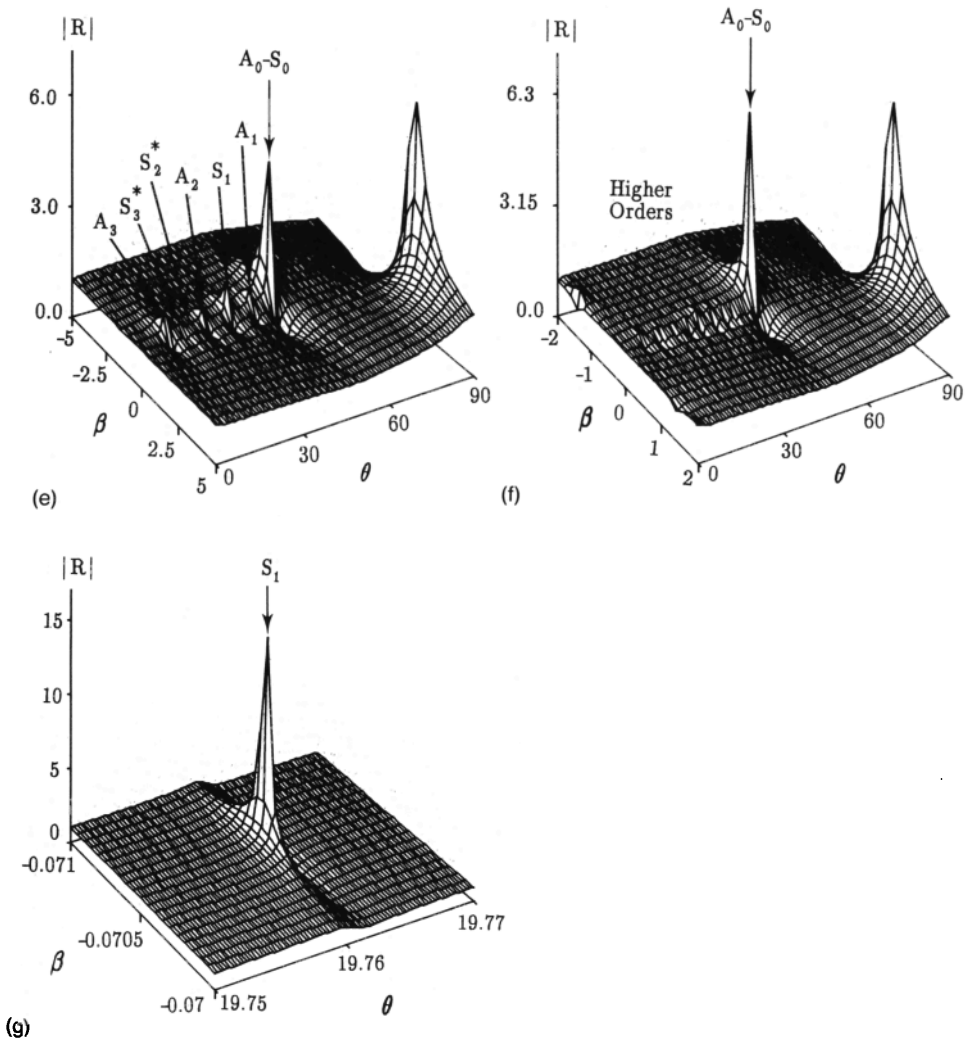

FIG. 5. (*Continued.*)

We also suppose that we can work at three different frequencies: 1, 2, and 5 MHz. The medium constants for water being $v_d=1480$ m/s, $\alpha_d=0.6\times10^{-18}$ s^2/mm, and $\rho=1.0$, we illustrate in Fig. 5 the theoretically calculated reflection moduli of heterogeneous waves for certain combinations of frequency and thickness. First of all, we note that the S_1 mode in part (b), and the S_2 and S_3 modes in parts (c)–(e) do not show up because of the nonzero grid dimensions. Nevertheless, these modes really exist, but correspond to extremely small heterogeneities and are located at precise angle positions as is illustrated in part (g) of the figure for the S_1 mode at $fd=2.5$ MHz mm. Second, we notice a small change in the three-dimensional representation of the complex harmonic wave reflection coefficient for different combinations of frequency and thickness at constant fd due to the assumed quadratic dependence of the absorption on the frequency.

At last, we assume that the effective width ($2W$) of the Gaussian profile insonifying the upper interface of the plate can be adjusted as we wish.

We first examine the influence of the beamwidth parameter W on the reflected profile and on the leaking energy contribution for fixed frequency and thickness. The heterogeneity characteristic of the complex harmonic waves in the decomposition of the incident profile being inversely proportional to the dimensions of the beam [Eq. (7)], the spacing between β_n and β_{n+1} and as a consequence also the range β_0 to β_{39} increases with decreasing W. Since the heterogeneity characteristic of the leaky component β_{Lw} does not change at fixed frequency and thickness, the dependence of β_n on the beamwidth W results, for larger W, in a shift of the peculiarities in the reflection coefficient toward higher summation index values n. As the coefficients A_n ($=A_{-n}$) are only significantly large for index values n up to 10 with a maximum for $n=5$, it is obvious that the incident decomposition will be most rigorously changed and the effect of leaky Lamb wave generation will be detectable only when these peculiarities are located in this region, in other words, when β_{Lw} belongs to the β_n's up to index value n equal to 10, or $|\beta_{\mathrm{Lw}}|<10/(1.9W)$. Therefore, it is essential to consider values of W smaller than $5.26/|\beta_{\mathrm{Lw}}|$. Larger values of the beamwidth result in a simple reduction of the amplitude of the Gaussian beam in reflection and in a negligible presence of energy leaking from the surface wave into the liquid. With A_n being maximum for $n=\pm5$, the optimum beamwidth to

produce strong leaky waves at θ_{Lw} must be situated at a value in the neighborhood of

$$W=2.63/|\beta_{Lw}|. \tag{10}$$

For the generation of the S_1 mode in a 1-mm brass plate at 5 MHz with $\theta_{Lw}=31.95°$ and $\beta_{Lw}=-0.345\ \text{mm}^{-1}$ (Fig. 6), the optimum beamwidth for strong Lamb wave generation is about 7.5 mm, where the leaky Lamb wave component at $x_r=0$ is maximal. And indeed, when we calculate the particle motions inside the plate due to the plate mode, we observe in Fig. 7 that the motions are most pronounced for $W=7.5$ mm, which means that in this case the Lamb wave can propagate over the largest distance inside the plate. For smaller or larger beam dimensions this propagation distance becomes smaller.

As a second observation, we notice that the reflected profile deformations plotted as a function of fractions of the beamwidth (x_r/W in horizontal axis) are most rigorous for the smallest incident profile dimensions although the power of the generated Lamb mode diminishes. This can be explained as follows: If the generated Lamb wave inside the plate is strong enough so that it still has a reasonable amplitude for $x>2W/\cos\theta$, it causes by interference a second lobe which extends the reflected profile beyond the specular reflection region. For large beamwidths, this distance can be too big so that no deformations occur. For smaller dimensions, there is a greater possibility for an extension of the specular reflection field. If however, the power of the generated Lamb wave for extremely small profiles is too small to be nonzero for $x>2W/\cos\theta$, the deformations again disappear. From our theoretical calculations, we generally could observe the largest extension of the trailing field (normalized to the beamwidth), caused by the leaking energy, for an ultrasonic beam with beamwidth parameter between

$$0.210/|\beta_{Lw}| \quad \text{and} \quad 0.526/|\beta_{Lw}|. \tag{11}$$

For the parameters used in Fig. 6, this corresponds to a range of 0.6 to 1.5 mm.

If we neglect the absorption effect in the liquid, we can translate the range given by (11) in terms of the parameter h mentioned earlier in the Introduction. Indeed, if $a_{0_{liq}}=0$, the imaginary part of the wave vector x component for which a Lamb wave is generated is equal to $-\beta_{Lw}\cos\theta_{Lw}$ ($=|\beta_{Lw}|\cos\theta_{Lw}$ in most cases). The parameter h is consequently given by

$$h=W|\beta_{Lw}|/2,$$

which corresponds for optimum beamwidth prediction to a range of values of h between 0.105 and 0.263. This result is in a very good agreement with the theoretical observations of Bertoni and Tamir[1] in the case of liquid/solid interfaces and generalizes these observations at the same time for plates (and other layered media).

In circumstances where one cannot experimentally observe the presence of the leaky Lamb wave from the reflected and transmitted fields,[10–11] although the dispersion curves predict its existence, the heterogeneous wave theory is a handy help to determine the optimum beamwidth pa-

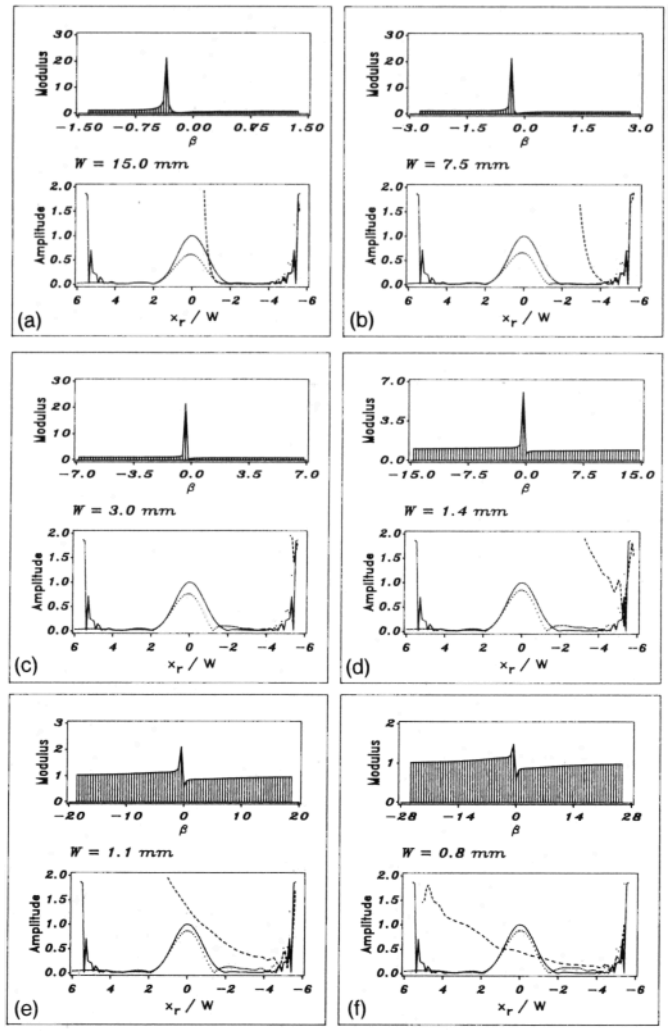

FIG. 6. Profile deformations (dotted line) and leaky wave contribution into the liquid (dashed line) after reflection of a Gaussian beam on a brass plate for variable width W of the profile. Fixed frequency $f=5$ MHz, thickness $d=1$ mm, and angle of incidence $\theta=31.95°$. The variations of the reflection moduli of the discrete heterogeneous waves that build up the incident profile are visualized above each illustration of profile deformation.

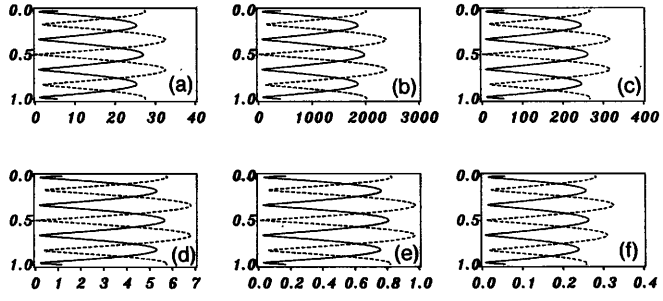

FIG. 7. Relative x (full line) and z (dashed line) Lamb wave displacement inside a 1-mm-thick brass plate at 5 MHz and 31.95° caused by the identical combination of heterogeneous waves which gives rise to the evanescent energy components in Fig. 6.

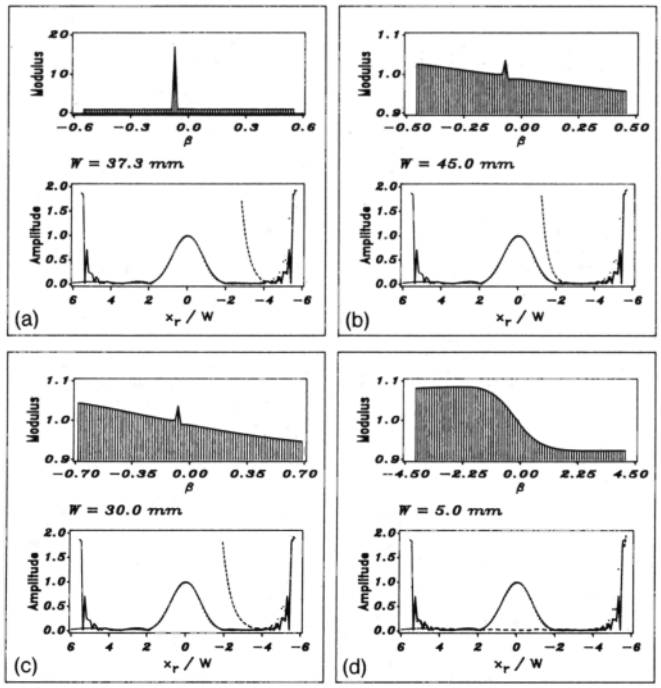

FIG. 8. Profile deformations and leaky wave contribution into the liquid after reflection of a Gaussian beam incident in the neighborhood of the "hidden" S_1-mode Lamb angle ($19.76° \approx \theta_{Lc}$) on a 0.5-mm brass plate at 5 MHz. (a) $W=37.5$ mm (optimum beamwidth), (b) $W=45$ mm, (c) $W=30$ mm, and (d) $W=5$ mm.

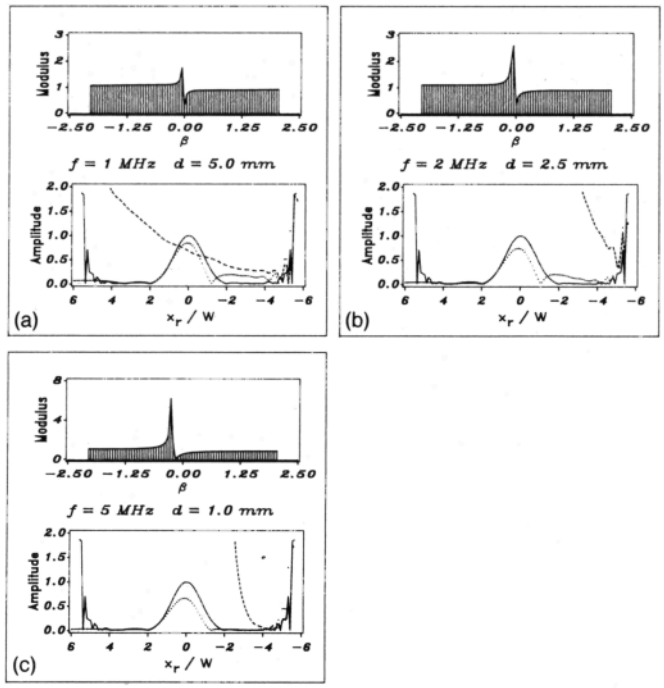

FIG. 10. Profile deformations and leaky wave contribution into the liquid after reflection of a Gaussian beam on a brass plate for fixed product $fd=5$ MHz mm. Fixed width $W=10$ mm and angle of incidence $\theta=23.4°$.

rameter for strongest Lamb wave generation inside a layer. For instance, the S_1-mode with Lamb angle near the longitudinal critical angle for a 0.5-mm brass plate at 5 MHz can easily be missed in experiments due to the fact that the pole corresponding to such a mode is located very close to the $\beta=0$ axis and can only be observed for a restricted range of incidence angles [Fig. 5(g)]. Because of the extremely small heterogeneity characteristic of the Lamb mode, the optimum beamwidth for strong Lamb wave generation is rather large (37.3 mm) (Fig. 8). Furthermore, the amplitudes of the particle motions inside the plate (which have to be considered as relative values for one beamwidth compared to another) are decreasing very fast for smaller or larger beamwidths (Fig. 9) so that, consequently, it is plausible that the Lamb wave inside the plate

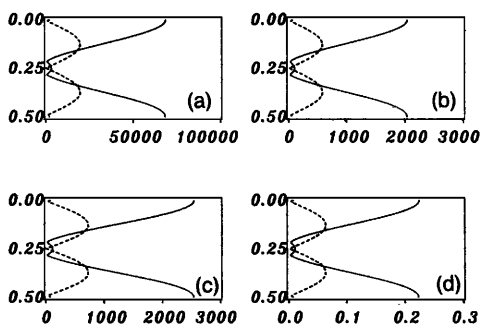

FIG. 9. Relative x and z Lamb wave displacement inside a 0.5-mm-thick brass plate at 5 MHz and 19.76° caused by the identical combination of heterogeneous waves which gives rise to the evanescent energy components in Fig. 8.

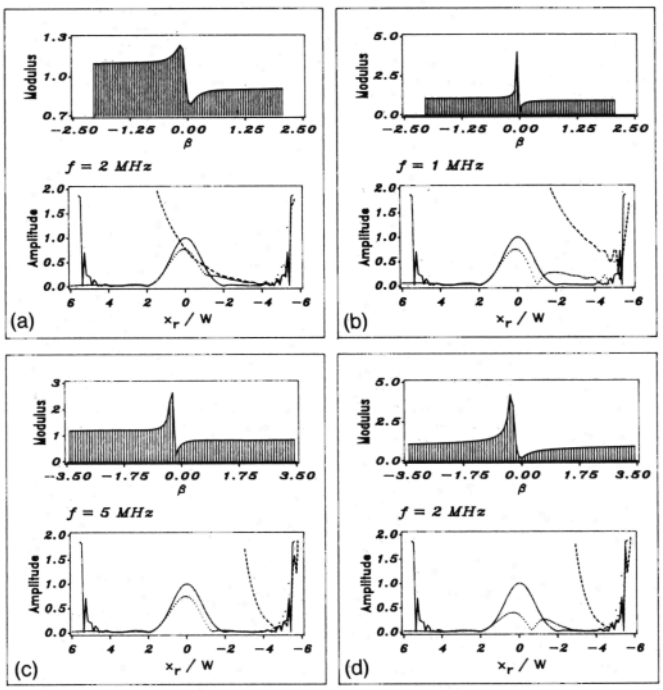

FIG. 11. Profile deformations and leaky wave contribution into the liquid after reflection of a Gaussian beam on a brass plate for variable frequency. (a) and (b) fixed width $W=10$ mm, thickness $d=2.5$ mm and angle of incidence $\theta=24°$. Generation of A_2 (case A) and A_1-plate modes (case B). (c) and (d) fixed width $W=6$ mm, thickness $d=1.0$ mm and angle of incidence $\theta=40°$. Generation of A_1 (case C) and S_0-plate modes (case D).

is never powerful enough to provoke a second lobe. This means that no deformation can be observed, even though (in optimal parameter circumstances) the Lamb wave can exist locally inside the plate over a considerable distance.

The three-dimensional plots shown in Fig. 5 illustrate very well the dependence frequency (f) and thickness (d) variations on the reflection coefficients for heterogeneous waves. First our attention goes to cases for which the product fd remains invariant, e.g., $fd=5$ MHz mm for $f=1$ MHz, $d=5$ mm or $f=2$ MHz, $d=2.5$ mm or $f=5$ MHz, $d=1$ mm. Figure 5(c)–(e) clearly illustrates that the positions of the critical angles for constant fd nearly do not change while the heterogeneity characteristics of the possible leaky Lamb wave are almost directly proportional to the frequency value. (Notice that we have to say "nearly" and "almost" because of the quadratic frequency dependence of the attenuation coefficients.)

An example of the effect of this feature on the reflection of an ultrasonic beam with fixed width $W=10$ mm, is shown in Fig. 10. The larger the f, the larger the range of heterogeneous waves in the original incident decomposition affected by a change in amplitude (and phase) after reflection. The consequences for the scattered profile and for the intensity of the leaking energy component in the liquid are analogous to the changes we observed for beamwidth variations at fixed frequency and thickness. We will explain the reason for this somewhat later.

When the thickness is kept constant and the frequency is variable (e.g., $d=2.5$ mm for 1 and 2 MHz or $d=1$ mm for 2 and 5 MHz), we observe a drastic change in the three-dimensional representation of the reflection coefficients of the heterogeneous waves (Fig. 5). The larger the f, the more Lamb waves can be generated at different angles. Furthermore, the detection position of the Lamb waves at low frequencies generally changes toward larger incidence angles for higher frequencies. Therefore, as the resonant conditions change at fixed incidence, it is obvious that the results for a Gaussian beam of constant dimension can be entirely different for one frequency compared to another and so it is perfectly possible, when applying different frequencies, to excite at the same angle a different Lamb wave with different heterogeneity characteristic. In Fig. 11(a) and (b), for instance, two different Lamb waves are excited by a Gaussian profile of 10 mm reflected on a brass plate of 2.5-mm thickness. At 2 MHz, the A_2 mode is generated, while at 1 MHz, the A_1 mode is generated. The respective displacements inside the plate are visualized in Fig. 12. The same phenomenon is illustrated in Fig. 11(c) and (d) where the reduction of frequency from 5 to 2 MHz for a 6-mm Gaussian beam at a 1-mm-thick plate results in the observance of the S_0 mode instead of the A_1 mode (see, also, Fig. 12).

Even if the width of the transducer is adjusted such that fW remains constant, one still observes drastic changes in the reflection phenomena (Fig. 13).

We now reverse the roles of frequency and thickness. Thickness variations at fixed frequency are very important in nondestructive evaluation of materials. Figure 5 again illustrates the changes in the heterogeneous wave reflection

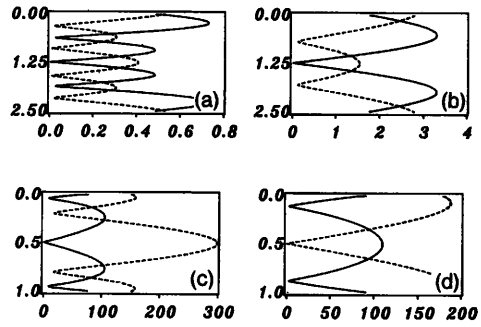

FIG. 12. Relative x and z Lamb wave displacement inside the different brass plates under the same circumstances as considered in Fig. 11.

coefficient. The effect of variable thickness is in fact the same as the effect frequency changes have on the scattering process. Angular positions of the Lamb modes change and, the larger the d, the more Lamb waves appear. Even for small variations of the thickness, one can observe considerable changes in the profiles as can be noticed from the sequence in Fig. 14. The smaller the thickness of the films, or the thickness variations of the layers, the higher the sound frequency must be in order to detect possible alterations in structure or geometry.

As was the case for frequency modifications, thickness variations can also have the effect that Lamb waves of a different nature are generated at the same angle for fixed beam dimension and frequency. By consequence, the profile deformations can differ one from another immensely. We illustrated this in Fig. 15 for a Gaussian beam of 8 mm at 2 MHz. The nature of the surface wave generated at 9.0° changes from S_1 (a negative group velocity Lamb wave[19]) to A_3 and to a higher-order mode which is not strongly present.

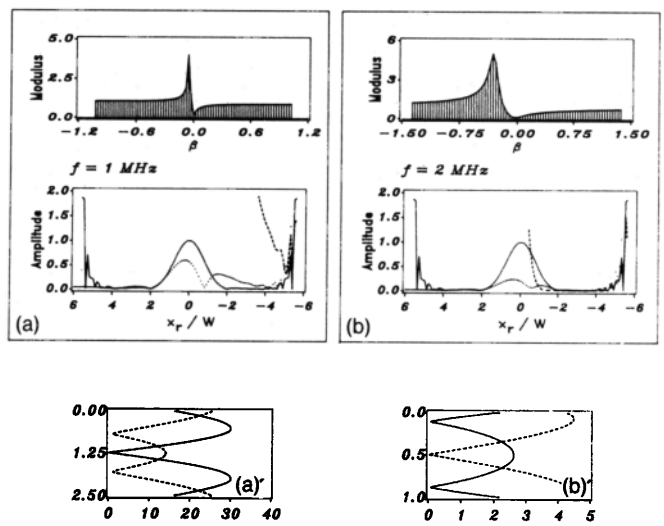

FIG. 13. Profile deformations and leaky wave contribution into the liquid after reflection of a Gaussian beam on a brass plate. Compare (a) and 11(a): fixed thickness $d=2.5$ mm, variable frequency and fixed fW product 20 MHz mm. Compare (b) and 11(c): fixed thickness $d=1.0$ mm, variable frequency and fixed fW product 30 MHz mm. The Lamb wave displacements corresponding to the situations in (a) and (b) are shown in the subfigures (a') and (b').

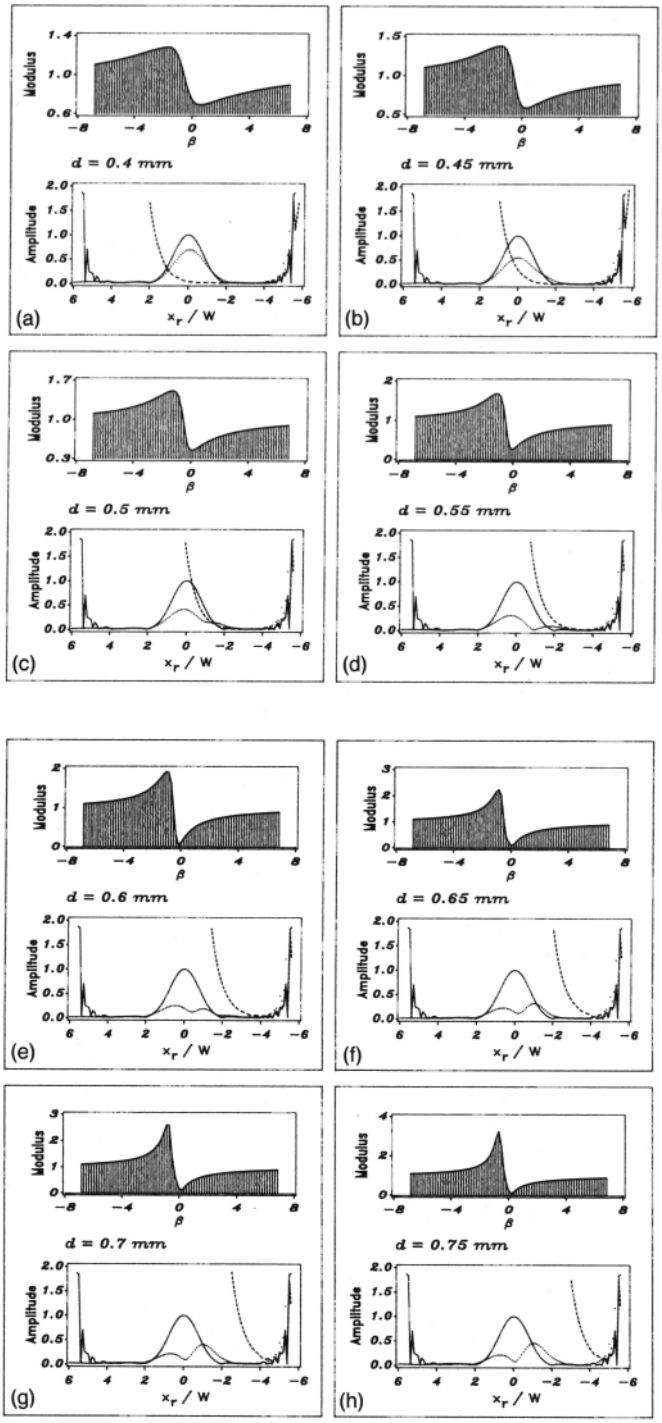

FIG. 14. Profile deformations and leaky wave contribution into the liquid after reflection of a Gaussian beam on a brass plate for variable thickness d of the plate. Fixed frequency $f=5$ MHz, width $W=3$ mm, and angle of incidence $\theta=47.5°$ (Rayleigh angle for water–brass interface).

In Fig. 16, we adjusted the beamwidth so that the relation d/W is the same as in Fig. 15(a). The drastic change is still present.

Figures 6–16 have taught us the following things. On one hand, we observe that beamwidth variations at fixed frequency and thickness produce different profiles because of a different intensity of the generated Lamb wave, which has the same heterogeneity characteristics for all values of the beamwidth. At fixed fd value and constant beamwidth

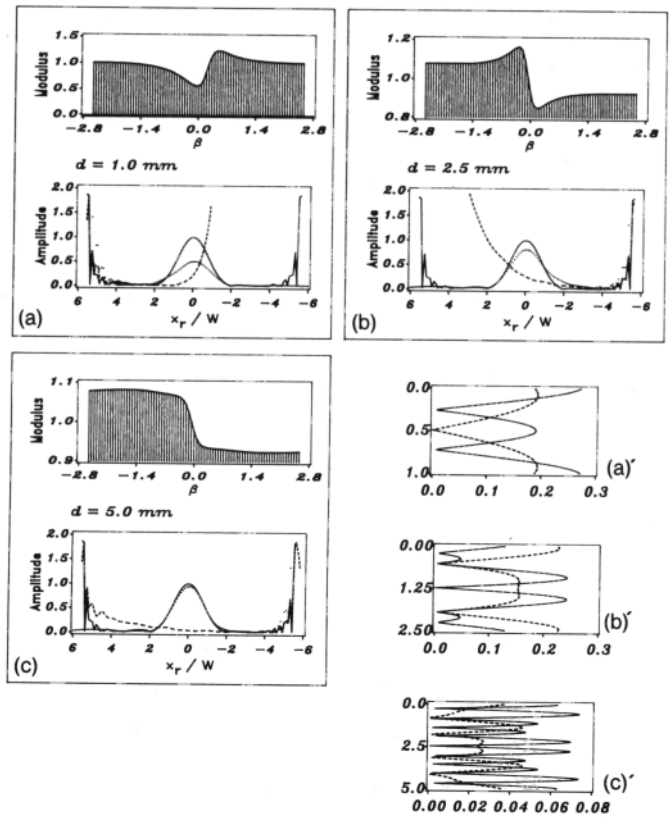

FIG. 15. Profile deformations and leaky wave contribution into the liquid after reflection of a Gaussian beam on a brass plate for variable thickness d of the plate. Fixed frequency $f=2$ MHz, width $W=8$ mm, and angle of incidence $\theta=9°$. The Lamb wave displacements corresponding to the situations in (a), (b), and (c) are shown in the subfigures (a′), (b′), and (c′). Generation of S_1 (case A and A′), A_3 (case B and B′) and higher-order antisymmetrical mode (case C and C′).

analogous results are obtained. For variable frequency and constant thickness or for variable thickness and constant frequency the reflected profiles of a Gaussian beam of given constant dimension changes drastically since other types of plate modes can be generated at the same angle, even if we adjust the beamwidth such that fW, respectively d/W, is invariant.

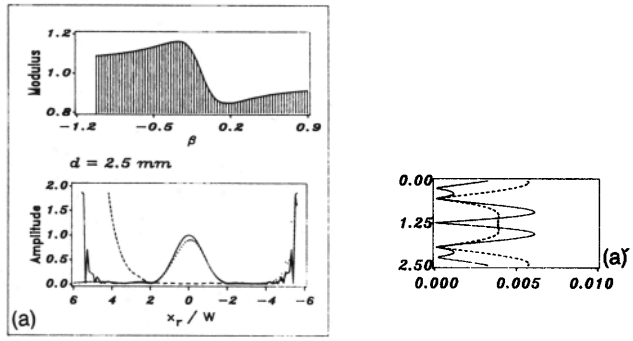

FIG. 16. Profile deformations and leaky wave contribution into the liquid after reflection of a Gaussian beam on a brass plate. Compare 16 and 15(a): fixed frequency $f=2$ MHz, variable thickness and fixed d/W relation: 1/8. The corresponding Lamb wave displacement is shown in the subfigure (a′).

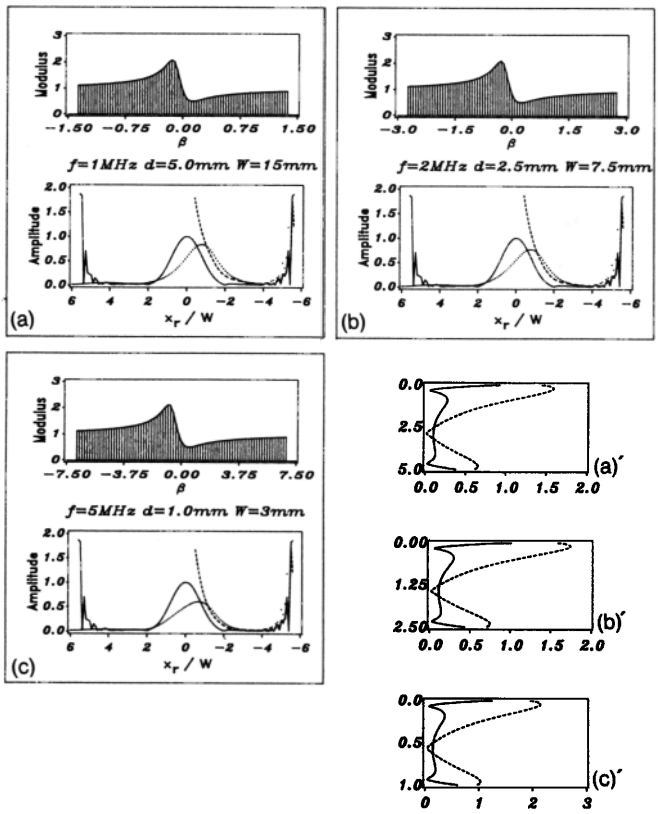

FIG. 17. Profile deformation and leaky wave contribution into the liquid after reflection of a Gaussian beam on a brass plate at 46°. The scattering phenomena and Lamb wave displacements are similar in all cases for which both products fd and fW are invariant: $fd=5$ MHz mm, $fW=15$ MHz mm. (a) and (a'): $f=5$ MHz, $d=1$ mm, and $W=3$ mm; (b) and (b'): $f=2$ MHz, $d=2.5$ mm, and $W=7.5$ mm; (c) and (c'): $f=1$ MHz, $d=5$ mm, and $W=15$ mm.

Especially from the case when $fd=$constant, illustrated in Figs. 6–10, we can resume this investigation with the following concluding statement:

Situations for which fd and fW are both constant lead to approximately the same profile deformations and to approximately the same indication of the presence or absence of a leaky wave.

Indeed, as fd is constant and assuming that the absorption is small, the frequency and thickness variations do not affect the angular positions of the Lamb waves in the plate. As fW is also constant, the complex harmonic waves in the decomposition change in heterogeneity characteristics inversely proportional to the beamwidth, but the peculiarities in the reflection coefficient of the various heterogeneous waves always occur at the same summation index value because of the (approximately) linear dependence of the poles of $|\mathbf{R}|$ on the frequency. A simple example for $fd=5$ MHz mm and $fW=15$ MHz mm is given in Fig. 17.

This statement also explains why the variations of the reflected profiles in Fig. 10 are comparable to the ones observed for variable beamwidth at fixed frequency and thickness:

The profile deformation in Fig. 10(a) for the ($f=1$ MHz, $d=5$ mm, $W=10$ mm) combination can also be obtained up to a large approximation level for ($f=2$ MHz, $d=2.5$ mm, $W=5$ mm) or even for ($f=5$ MHz, $d=1$ mm, $W=2$ mm). The situation in Fig. 10(b) is almost identical to the combinations ($f=1$ MHz, $d=5$ mm, $W=20$ mm) and ($f=5$ MHz, $d=1$ mm, $W=4$ mm), and finally the same reflection phenomena visualized in Fig. 10(c) also occur for ($f=1$ MHz, $d=5$ mm, $W=50$ mm) and ($f=2$ MHz, $d=2.5$ mm, $W=25$ mm). This means in fact that Fig. 10 at the same time illustrates the influence of beamwidth variations at 5 MHz on plate 1 (1 mm) for $W=2$, 4, and 10 mm, at 2 MHz on plate 2 (2.5 mm) for $W=5$, 10, and 25 mm and at 1 MHz on plate 3 (5 mm) for $W=10$, 20, and 50 mm.

Note that, when the plate thickness becomes much larger than the wavelength (i.e., $fd\rightarrow+\infty$), the properties of the plate tend toward the characteristics of a half-space. Similar nonspecular effects then occur for each situation in which fW is an invariant.

It is not necessary to perform the calculations, to see from the basic principles of our heterogeneous wave decomposition model that the previous statement can be generalized for an m-layered medium with thicknesses d_i (i:1$\cdots m$) in the following way:

Situations for which fd_i (i:1$\cdots m$) and fW are constant lead to approximately the same profile deformations and to approximately the same indication of the presence or absence of a leaky wave.

This result can be very interesting for NDT laboratory research on scale models, for instance to study thick ice covers in the Arctic.

III. CONCLUSIONS

We have shown that, apart from the angle of incidence, thickness of the considered material together with frequency and effective beamwidth of the ultrasonic bounded beam are three very important parameters in the nondestructive investigation of plates immersed in water. Therefore, we used a model based on the scattering of heterogeneous waves at plane interfaces. From the principles of this model, we were able to predict a range of values for the beamwidth of the incident wave for which nonspecular reflection and transmission effects in the scattered intensity distribution profile have to be expected. Moreover, for a given (f,d) combination, optimum values of the incident profile dimension close to the interface of the plate can be determined in order to generate strong leaky Lamb waves of a particular mode. The effects of frequency and thickness variations are discussed and examples are provided. Especially the leaky Lamb wave component provides extremely interesting information that is of great importance in the field of acoustic microscopy research and can be used in inverse problem techniques by comparison with the theoretically obtained three-dimensional representation of the heterogeneous wave reflection coefficients. We also found that different situations can result in similar nonspecular effects (deformations and leaky wave contribution) if certain conditions concerning the three parameters f, d, and W are satisfied. This is the case in all situations where the width of the ultrasonic beam and the

thickness of the plate expressed in units of wavelength is the same: a result which can be interesting for laboratory investigations on scale models.

[1] H. L. Bertoni and T. Tamir, "Unified Theory of Rayleigh-Angle Phenomena for Acoustic Beams at Liquid–Solid Interfaces," Appl. Phys. **2**, 157–172 (1973).

[2] T. J. Plona, M. Behravesh, and W. G. Mayer, "Rayleigh and Lamb Waves at Liquid–Solid Boundaries," Ultrasonics Proc. 171–174 (July 1975).

[3] L. E. Pitts, T. J. Plona, and W. G. Mayer, "Theoretical Similarities of Rayleigh and Lamb Modes of Vibration," J. Acoust. Soc. Am. **60**, 374–377 (1976).

[4] T. J. Plona, L. E. Pitts, and W. G. Mayer, "Ultrasonic Bounded Beam Reflection and Transmission Effects at a Liquid/Solid–Plate/Liquid Interface," J. Acoust. Soc. Am. **59**, 1324–1328 (1976).

[5] M. A. Breazeale, L. Adler, and G. W. Scott, "Interaction of Ultrasonic Waves Incident at the Rayleigh Angle onto a Liquid–Solid Interface," J. Appl. Phys. **48** (2), 530–536 (1977).

[6] T. D. K. Ngoc and W. G. Mayer, "Numerical Integration Method for Reflected Beam Profiles near Rayleigh Angle," J. Acoust. Soc. Am. **67**, 1149–1152 (1980).

[7] T. D. K. Ngoc and W. G. Mayer, "A General Description of Ultrasonic Nonspecular Reflection and Transmission Effects for Layered Media," IEEE Trans. Sonics Ultrasonics **SU-27** (5), 229–236 (1980).

[8] T. Kundu, "On the Nonspecular Reflection of Bounded Acoustic Beams," J. Acoust. Soc. Am. **83**, 18–24 (1988).

[9] T. Kundu, A. K. Mal, and R. D. Weglein, "Calculation of the Acoustic Material Signature of a Layered Solid," J. Acoust. Soc. Am. **77**, 353–361 (1985).

[10] M. de Billy and I. Molinero, "On the Nonobservance of Nonspecular Bounded Beam Reflection Effects of Lamb Modes," J. Acoust. Soc. Am. **83**, 1249–1254 (1988).

[11] I. Molinero, "Contribution à létude de la diffusion acoustique par des plaques et des fils en incidence oblique; Génération d'ondes de surface et d'ondes guidées," Ph.D. thesis, Université Paris VII (1987).

[12] J. M. Claeys and O. Leroy, "Reflection and Transmission of Bounded Sound Beams on Half-Spaces and through Plates," J. Acoust. Soc. Am. **72**, 585–590 (1982).

[13] K. Van Den Abeele and O. Leroy, "Complex Harmonic Wave Scattering as the Framework for Investigation of Bounded Beam Reflection and Transmission at Plane Interfaces and its Importance in the Study of Vibrational Modes," J. Acoust. Soc. Am. **93**, 308–323 (1993).

[14] K. Van Den Abeele, "Alternative Fundamental Theoretical Descriptions for Acousto-optic and Acoustic Investigation of Pulsed and Profiled Ultrasound in View of Nondestructive Testing of Layered Structures," Ph.D. thesis, K. U. Leuven Campus Kortrijk (1992)

[15] M. Deschamps and C. Changlin, "Réflexion-Réfraction de l'Onde Plane Hétérogène: Lois de Snell–Descartes et Continuité de l'Energie," J. Acoust. **2**, 229–240 (1989).

[16] B. Poirée, "Complex Harmonic Plane Waves," in *Proceedings of the Symposium on Physical Acoustics: Fundamentals and Applications*, Kortrijk, Belgium, edited by O. Leroy and M. Breazeale (Plenum, New York, 1990), pp. 99–117.

[17] M. Deschamps, "L'Onde Plane Hétérogène et ses Applications en Acoustique Linéaire," J. Acoust. **4**, 269–305 (1991).

[18] L. M. Brekhovskikh, *Waves in Layered Media* (Academic, New York, 1960).

[19] J. Wolf, T. D. K. Ngoc, R. Kille, and W. G. Mayer, "Investigation of Lamb Waves Having a Negative Group Velocity," J. Acoust. Soc. Am. **83**, 122–126 (1988).